*materials*

**MDPI**

*Article*

# Enhancing the Energy Density of Tricritical Ferroelectrics for Energy Storage Applications

**Li He [1], Yan Wang [2], Jinghui Gao [2,*](ID), Jianhong Wang [1], Tongxin Zhao [2], Zhixin He [2], Zuting Zhong [1], Xingmin Zhang [3,*] and Lisheng Zhong [2,*](ID)**

[1] School of Automation and Information Engineering, Xi'an University of Technology, Xi'an 710048, China; heli@xaut.edu.cn (L.H.); 2170320069@stu.xaut.edu.cn (J.W.); 3160434039@stu.xaut.edu.cn (Z.Z.)

[2] State Key Laboratory of Electrical Insulation and Power Equipment, Xi'an Jiaotong University, Xi'an 710049, China.; wangyan0616@stu.xjtu.edu.cn (Y.W.); ztx1021@stu.xjtu.edu.cn (T.Z.); hezx24@stu.xjtu.edu.cn (Z.H.)

[3] Shanghai Synchrotron Radiation Facility, Shanghai Advanced Research Institute, Chinese Academy of Sciences, Shanghai 201204, China

[*] Correspondence: gaojinghui@mail.xjtu.edu.cn (J.G.); zhangxingmin@sinap.ac.cn (X.Z); lszhong@mail.xjtu.edu.cn (L.Z.)

check for updates

**Abstract:** Recently, tricritical ferroelectrics have been drawn tremendous attention, owing to their ultrahigh dielectric permittivities of up to $\varepsilon_r > 5 \times 10^4$, and their consideration for prototype materials in the development of high-performance energy storage devices. Nevertheless, such a materials system suffers from the disadvantage of low breakdown strength, which makes its energy density far from the satisfactory level for practical application. In this paper, a material-modification approach has been reported, for improving the dielectric strength for tricritical ferroelectric materials $Ba(Ti_{1-x}Sn_x)O_3$ (BTS) through doping with $Bi_{1.5}ZnNb_{1.5}O_7$ (BZN) additives. The results suggest that the electric strength has been largely improved in the modified tricritical ferroelectric material ($BTS_x$-$y$BZN), and the associated energy density reaches $U_e = 1.15 \text{ J/cm}^3$. Further microstructure investigation indicates that the modified tricritical ferroelectric material exhibits homogenous fine grains with perovskite structure in crystal symmetry, and the BZN may help to form a special structure that could enhance the breakdown strength. The findings may advance the material design and development of high-energy storage materials.

**Keywords:** ferroelectric material; tricriticality; energy density; breakdown strength

## 1. Introduction

Owing to the ultrafast response of spontaneous polarization with an external electric field, smart material ferroelectrics are considered to be a type of advanced energy storage material, and they can be used for energy harvesting, due to their capacity for rapid storage or release of energy [1,2], and they have possible applications as high-power-density capacitor devices [3,4]. However, such a material system suffers from a disadvantage of low energy density, which limits its utilization as an energy storage device. Therefore, tremendous effort has been made to enhance the energy density for ferroelectric materials [5,6].

The energy density that is stored in ferroelectric material can be reflected by the relationship $u_e = \int E dD = \varepsilon_0 \int E d\varepsilon_r E$, where $E$ stands for the electric field strength, and $\varepsilon_r$ means the relative dielectric permittivity. These parameters ($E$ and $\varepsilon_r$) are two decisive factors for the magnitude of energy density in ferroelectric devices. Recent investigation has reported an ultrahigh dielectric response with a large relative permittivity of $\varepsilon_r \approx 2 \sim 5.4 \times 10^4$ in a thermodynamically-special tricritical point, which is tens or thousands of times greater than normal ferroelectric dielectrics,

and thus there is a promising future for the potential applications of energy storage devices [7–10]. Nevertheless, the maximum energy density for tricritical ferroelectrics reported up till now only reaches 30 mJ/cm$^3$, which is far below the satisfactory level for practical utilization. It should be noted that main reason for such a drawback is that tricritical ferroelectrics usually exhibit a low breakdown strength, which hinders their application at high electric field strength, making such an ultrahigh-permittivity material system futile for energy storage devices. The central issue to overcoming such a barrier is how to effectively enhance the electric breakdown strength for tricritical ferroelectrics. In the case of dielectric ceramics, tremendous attempts have been made to improve the breakdown phenomenon through various methods. Wang et al., Xie et al. and Zhao et al. studied the role of dopants, such as yttrium, magnesium, gallium, silicon, and silver, in improving the dielectric strength, and thus the energy storage performance of barium titanate-based and correlated materials [11–13], and further studies have pointed out the importance of forming a core–shell morphology in the system [14,15]. On the other hand, some work also focused on enhancing the breakdown strength for barium titanate or barium strontium titanate materials, through adding glass into the system [16–18]. In addition, intensive studies were performed on forming composite materials with polymers for barium titanate and correlated systems [19–21]. Although studies on tricritical ferroelectric and its energy storage properties have been quite limited at present, there is no reason that the above-mentioned approaches on improving energy density should be inapplicable to tricritical ferroelectric materials.

In this paper, we propose a material-modification strategy to enhance the energy density for the tricritical ferroelectric material Ba(Ti$_{1-x}$Sn$_x$)O$_3$ (BTS) through doping with Bi$_{1.5}$ZnNb$_{1.5}$O$_7$ (BZN) additives [22–24]. In order to clarify the effect of BZN on sintering conditions, the density of BTS$x$-$y$BZN has been measured with different sintering temperatures. With the purpose of studying the microstructure and crystal structure of this doped material, scanning electron microscopy (SEM) and synchrotron X-ray diffraction (XRD) have been performed for BTS$_{x-y}$BZN ceramics. Also, the role of tricritical transition on the dielectric response for BZN-doped BaTiO$_3$–based ceramics has been investigated, by employing the thermal spectrum of dielectric permittivity for the compositions across the tricritical point. Furthermore, the electric breakdown strength has been evaluated by measuring the polarization (*P*)-electric field (*E*) curves, and comparing the energy storage and energy efficiency of different compositions of BTS$_{x-y}$BZN. The findings may provide a guideline for developing advanced ferroelectrics with large capacities energy storage, and ultrahigh energy efficiency.

## 2. Materials and Methods

The chemical reagents used are analytical reagent grade (≥99%) produced by Sinopharm Co., Ltd. China. Samples of (1−$y$)Ba(Ti$_{1-x}$Sn$_x$)O$_{3-y}$Bi$_{1.5}$ZnNb$_{1.5}$O$_7$ (BTS$_x$-$y$BZN, $x$ = 0.05, 0.105, 0.15, 0.2; $y$ = 5 wt %, 10 wt %, 15 wt %, 20 wt %) were all fabricated with the conventional solid reaction method. For Ba(Ti$_{1-x}$Sn$_x$)O$_3$ ceramics, raw powders of BaCO$_3$, SnO$_2$, and TiO$_2$ were first weighed according to the calculated stoichiometric ratio ($x$ = 0.05, 0.105, 0.15, 0.2). The mixtures were then ball-milled with anhydrous ethanol for four hours. After being dried in the oven, the samples were calcined in a furnace at 1300 °C for four hours, and then ground into powder. As for the Bi$_{1.5}$ZnNb$_{1.5}$O$_7$ ceramics, raw powders of Bi$_2$O$_3$, ZnO, and Nb$_2$O$_5$ were weighed, then ball-milled for four hours, and calcined at 800 °C for two hours. With the calculated mixture ($y$ = 5 wt %, 10 wt %, 15 wt %, 20 wt %) of prepared BTS and BZN powders, another ball-milling process of eight hours was conducted. Then, 10 wt % polyvinyl alcohol (PVA) was added as a binder. The samples were pressed in a mold, and were obtained after sintering at a series of temperatures of 1025 °C, 1050 °C, 1075 °C, 1100 °C, and 1125 °C for two hours. Finally, two parallel sides of the samples were sputtered with Au electrodes for further measurements.

The crystal structure information was investigated by the synchrotron X-ray diffraction method at beamline 14B1 of the Shanghai Synchrotron Radiation Facility. The specimens were milled into fine powders, and measurements were performed with a photons beam with an energy level of

10 keV. Observations of microstructure and grain size was carried out by scanning electron microscopy (SEM SU3500, HITACHI, Tokyo, Japan). The temperature-dependence of dielectric permittivity was measured by a testing system consisting of a LCR HITESTER (IM3536, Hioki, Nagano, Japan), a Keithley 2000 meter, a Delta chamber, and a set of computers. The LCR HITESTER applies a small alternating current (AC) field with an amplitude of 1 V, at various frequencies on the sample, and it measures the capacity by testing the electrical current. The dielectric permittivity was calculated from the capacity and the dimensions of sample. The Keithley 2000 was used to record the temperature of the sample during the heating or cooling process. Both the LCR and the Keithley were connected to the computer through GPIB interfaces. As for the characterization of energy storage performance, polarization (*P*), electric field (*E*), and hysteresis loop were measured by using a ferroelectric workstation (PK-CPE1701, PolyK, Philipsburg, PA, USA) equipped with a heating specimen stage, and all of the specimens were tested at 40 °C, which is the tricritical point temperature for $BTS_{0.105}$.

## 3. Results and Discussion

### 3.1. Density

Figure 1 presents the bulk density curves of the $BTS_{0.105-}y$BZN ceramics sintered from 1025 °C to 1125 °C. It is obvious that the density change strongly depends on the BZN content, as well as the sintering temperature. It is reported that the sintered $BTS_{0.105}$ ceramic has a bulk density of 6.04 g/cm$^3$, with a relative density of 98% at 1380 °C [25], while the BZN ceramic has a lower sintering temperature at 950 °C [26]. Thus, the increase of the BZN doping in the $BTS_{0.105}$ ceramics could effectively lower the sintering temperature. It can be seen in Figure 1 that with 10 wt % BZN added, the optimum sintering temperature of $BTS_{0.105}$-10BZN can be lowered to 1100 °C. The dense and well-sintered $BTS_{0.105-}y$BZN($y$ = 10 wt %) ceramics showed a high relative density that was higher than 98%. According to such a result, sintering conditions of 1100 °C, 2 hr were used for the specimen, for further measurements.
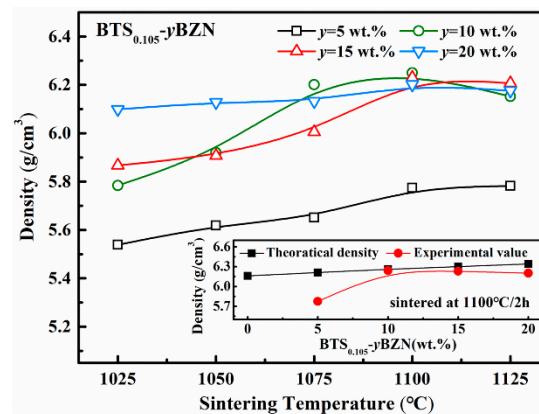


**Figure 1.** The change of density for $BTS_{0.105-}y$BZN ceramics ($y$ = 5 wt.%, 10 wt.%, 15 wt.%, 20 wt.%) with respect to the sintering temperature. The inset shows the comparison between the theoretical and experimental densities.

### 3.2. SEM

Figure 2 shows the SEM micrographs of the $BTS_{0.105}$-$y$BZN ceramics with different amounts of BZN, from 5 wt % to 20 wt %. The particle sizes of both $BTS_{0.105}$ and BZN mixing powders after the ball milling process, were about 0.5 μm. According to previous studies, the 950 °C-sintered BZN showed a large grain size of about 10 μm [25,26]. The optimum 1100 °C sintering temperature was higher than that of the BZN (950 °C) [26], but much lower than that of the BZN (1380 °C) [25]. However, no abnormal large BZN grain could be observed in Figure 2. The grain size of each specimen

was measured, and the grain size increased from about 0.5 μm to 4 μm, with the BZN content increasing from 5 wt % to 20 wt %. As shown in Figure 2a, large amounts of porosities appeared in the grain boundary, while the dense sintered $BTS_{0.105}$-$y$BZN ceramics (Figure 2b–d) exhibited apparent concrete-like morphologies, with uniform $BTS_{0.105}$ grains surrounded by BZN existing in the grain boundary.
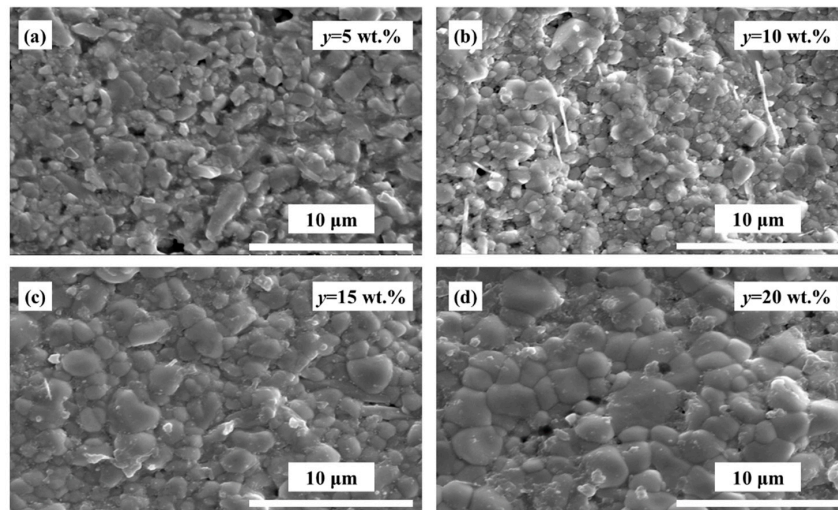


**Figure 2.** Scanning electron microscopy (SEM) images of the surface morphology for as-grown $BTS_{0.105}$-$y$BZN ceramics (**a**) $y$ = 5 wt %; (**b**) $y$ = 10 wt %; (**c**) $y$ = 15 wt %; (**d**) $y$ = 20 wt %.

*3.3. High-Resolution X-Ray Diffraction*

With the aim of detecting the crystal structure for the $BTS_{0.105-y}$BZN system, a high-resolution X-ray diffractometer with a powerful synchrotron light source was employed. The pure $BTS_{0.105}$ with no BZN doping was also scanned as a reference. As shown in Figure 3, the XRD result of $BTS_{0.105}$ suggest that it exhibits a typical perovskite structure for normal ferroelectric material, and the enlarged figure shows a singular peak with no peak splitting. On the other hand, the XRD spectrum for $BTS_{0.105-y}$BZN ($y$ = 10 wt %) specimen also shows similar peaks with $BTS_{0.105}$, which suggests that $BTS_{0.105-y}$BZN ($y$ = 10 wt %) exhibits perovskite structure, and there is no obvious BZN phase in the specimen. Moreover, the enlarged reflection shows apparent peak splitting, which means that BZN enters into the lattice of $BTS_{0.105}$ and slightly modifies the dimension of the $BTS_{0.105}$ unit cell. It should be noted that such peak splitting is different from the one in ferroelectric tetragonal, orthorhombic, or rhombohedral symmetry, because it does not vary with different reflections.
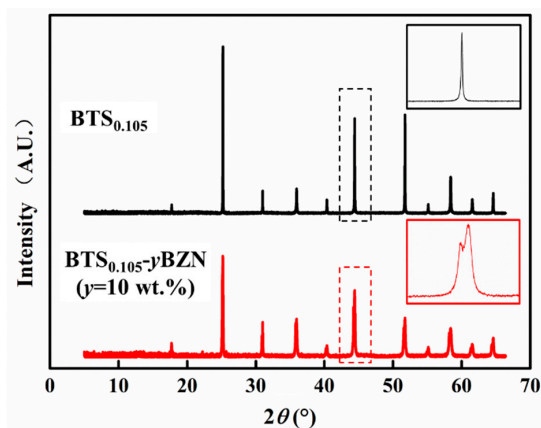


**Figure 3.** High-resolution X-ray diffraction results for $BTS_{0.105}$ and $BTS_{0.105-y}$BZN($y$ = 10 wt %). Each enlarged reflection is shown in the inset.

## 3.4. Dielectric Response

In order to discuss the role of tricritical transition on the dielectric response for BZN-doped BaTiO$_3$–based ceramics, the thermal spectrum of dielectric permittivity for the specimens has been measured with the composition across the tricritical composition. The tricititical transition [27–30], which is the crossover point between the first-order and second-order phase transition, manifests itself as the enhancement of the dielectric permittivity maximum at Curie temperature when the composition or stress is approaching to it [31]. Originally, the tricritical point has been reported in BaTiO$_3$ and PbTiO$_3$ systems under hydrostatic pressure [32,33]. Later, such a phenomenon has been reported in the composition–temperature phase diagram of the Pb(Zr$_{1-x}$Ti$_x$)O$_3$ (PZT) system [34]. A recent investigation on the high-performance BaTiO$_3$-based ceramics suggests that a large dielectric response with the maximum permittivity $\varepsilon_r$ > 20000 appeared at the Curie temperature of tricritical composition [7,8]. Further studies reveal that higher dielectric permittivities ($\varepsilon_r$ = 45000 ~ 54000) can be achieved in the tricritical point of BTS and Ba(Ti$_{1-x}$Hf$_x$)O$_3$ (BTH) ceramics [9,10,35]. The temperature-dependence of dielectric permittivity for BTS$x$-10BZN is shown in Figure 4. It can be seen that when the composition approaches the tricritical point at $x$ = 0.105, the dielectric permittivity reaches to the maximum peak value of 1264. Therefore, the results verify that the BZN addition has not changed the tricritical point composition of the BTS system. It should be noted that the pure BZN system showed a relatively low dielectric permittivity of around 100~160 for thick film, as well as ceramics, as reported by Wang's group [23,24], and therefore the addition of tricritical ferroelectric material can largely enhance the dielectric permittivity for the material system. In addition, the dielectric loss tan$\delta$ for all of our specimens was less than 5% in a temperature range of $-50$ °C to 100 °C, and a frequency range of $10^2 - 10^5$ Hz.
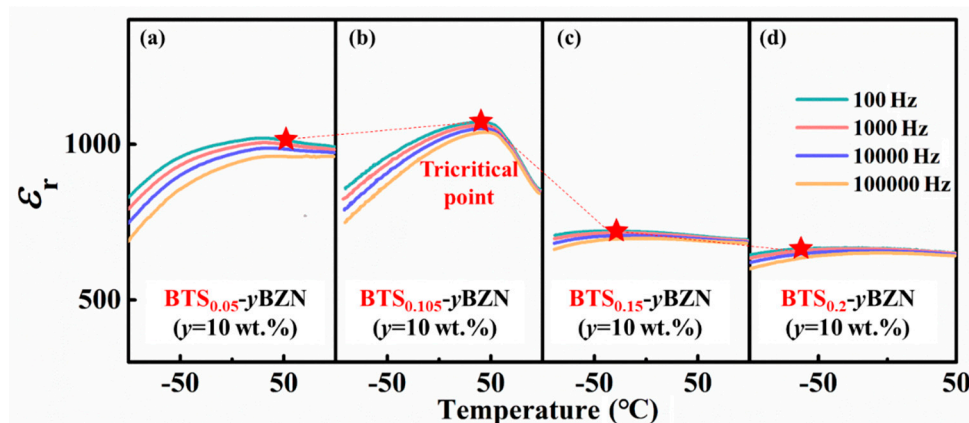


**Figure 4.** Temperature-dependence of dielectric permittivity for BTS$_x$-$y$BZN ($y$ = 10 wt %) (**a**) $x$ = 0.05; (**b**) $x$ = 0.105; (**c**) $x$ = 0.15; (**d**) $x$ = 0.2 at different testing frequencies ($f$ = $10^2$, $10^3$, $10^4$, $10^5$ Hz). $x$ = 0.105 shows the maximum peak value, indicating the tricritical behavior for this composition.

## 3.5. Electric Breakdown

In order to evaluate the role of BZN on tuning the electric breakdown for the barium titanate ceramic system, the AC breakdown strength test was performed for BTS$_{0.105-y}$BZN ceramics with different BZN contents. Wu et al. reported that the addition of BZN could largely enhance the dielectric strength of pure BaTiO$_3$ ceramics [22]. This study suggests that such a method is also effective in the case of tricritical ferroelectrics. The breakdown behavior for tricritical ferroelectrics has been analyzed by using a two-parameter Weibull distribution relationship: $P = 1 - \exp(-E/E_b)$, where $E$ is the tested breakdown strength, and $P$ is the possibility of electric failure. $E_b$ and $\beta$ are the scale and shape parameters, which describe the statistical dielectric strength and the dispersion of the data, respectively. The tested results are shown in Figure 5. The BTS$_{0.105}$ ceramic without the addition of BZN showed a relatively low breakdown strength of $E_b$=148 kV/cm (with the shape parameter

$\beta$ = 8.16). When adding 5 wt % content of BZN, the breakdown strength of the specimen rose to $E_b$ = 199 kV/cm (with the shape parameter $\beta$ = 8.84). On further increasing the content of BZN to 10 wt %, the breakdown strength will be enhanced to a maximum value of $E_b$ = 233 kV/cm. It is obvious that the addition of BZN can effectively enhance the breakdown strength by 57% for tricritical ferroelectric BTS$_{0.105}$ materials. It is highly possible that the addition of BZN, exhibiting an intermediate dielectric permittivity ($\varepsilon_r$ = 30 ~ 160), is able to smooth the electric field distribution around the high-permittivity tricritical-ferroelectric grains [23]. Further increasing the BZN content to 15 wt % or 20 wt % will lead to a slight decrease of dielectric strength, with $E_b$ = 232 kV/cm and 199 kV/cm, respectively. The possible reason may lie in the slight drop of density with the addition of BZN. It can thus be concluded that BZN additives can effectively enhance the breakdown strength for tricritical ferroelectrics.
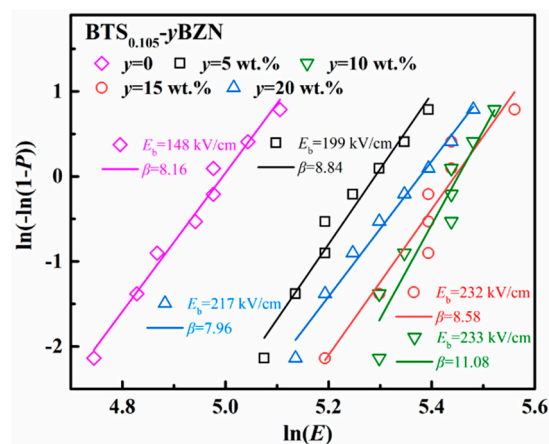


**Figure 5.** Weibull analysis for the BTS$_{0.105-y}$BZN ceramics ($y$ = 5 wt %, 10 wt %, 15 wt %, 20 wt %) describing the electric strength for the materials.

### 3.6. Energy Density and Energy Efficiency

The energy storage performance for the BTS$_{0.105-y}$BZN ceramics can be evaluated by measuring the polarization-electric field curves (known as *P-E* hysteresis loops) for the specimens. As shown in Figure 6a, the *P-E* loop for BTS$_{0.105}$ without BZN doping shows a large maximum polarization of $P_{max} \approx 23$ $\mu$C/cm$^2$, but the specimen can withstand a relatively low electric field strength, and the polarization saturates at a comparably low field region. With an increase in the BZN content, although the maximum polarization decreases to less than 10 $\mu$C/cm$^2$, the maximum electric field increases.

In order to further qualify the energy performance for the BTS-BZN system, the energy density for the BTS$_{0.105}$-$y$BZN specimens has been calculated by the integration of the *P-E* curve with respect to the electric field from $P_{max}$ to $P_r$, which is an indication of energy that can be release from the material with the removal of the electric field. As shown in Figure 6b, all of the compositions show a similar tendency for the energy density to increase with an increase of the electric field, and the maximum value of energy density for this material system appears at a composition of $x$ = 0.105, $y$ = 10 wt %, and the energy density value can reach to $U_e$ = 1.15 J/cm$^3$. Such a result is slightly higher than the previously-reported BT-BZN system, with a maximum discharging energy density of 0.8 J/cm$^3$, as reported by Wu L.W. et. al [22]. Although such a level of energy density is lower than the polymer/BaTiO$_3$ composite materials (with an energy density of around 7 J/cm$^3$ [21,36]), it can still be considered as one of the more promising ceramic capacitor materials, since the value is superior to the value ($U_e$ < 0.035 J/cm$^3$) that was first reported in BTS$_{0.105}$ ceramics [9], which indicates the possibility for tricritical ferroelectrics as a promising material system for future energy storage devices.
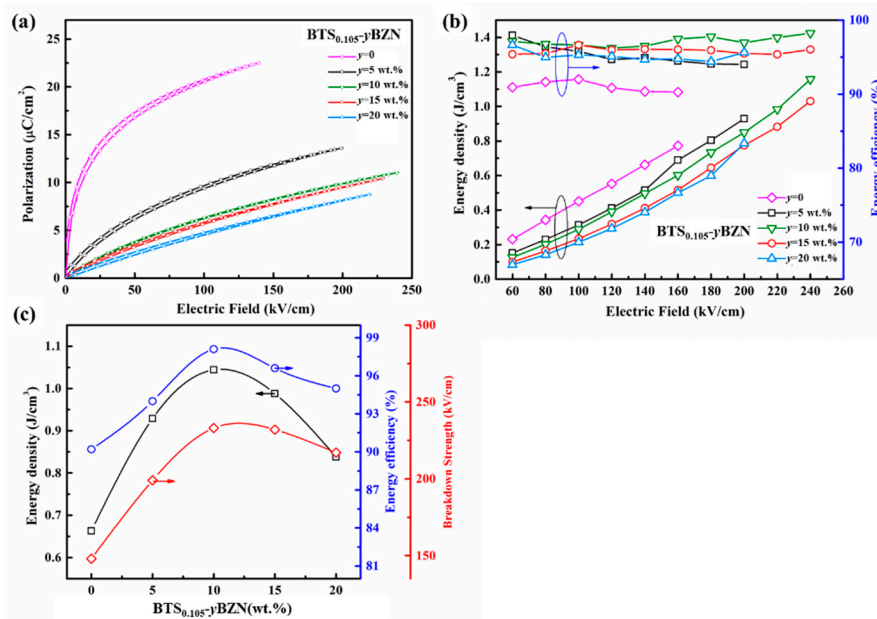
**Figure 6.** The energy storage properties for BTS$_{0.105-y}$BZN ($y$ = 5 wt %, 10 wt %, 15 wt %, 20 wt %) ceramics. (**a**) *P-E* hysteresis loops; (**b**) electric field strength-dependence of energy density and efficiency; (**c**) The change of breakdown strength, energy density, and efficiency with BZN content.

The composition dependence of energy density, breakdown strength, and efficiency has been shown in Figure 6c. It can be seen that the breakdown strength firstly increases and then decreases with the increase of BZN content, and the optimal breakdown strength is found at a BZN content of 10 wt %. Concerning the composition-dependence of energy storage performance, it shows a similar tendency to breakdown strength, and the maximum energy density appears at a BZN content of 10 wt %. The consistency between the $U_e$ and $E_b$ suggests that the energy density of tricritical ferroelectrics is effectively improved through enhancing the breakdown strength via the addition of BZN. Furthermore, such a BTS$_{0.105-y}$BZN material system shows a high efficiency of up to 99%, which confirms the advantage for the possible application of tricritical ferroelectrics.

## 4. Conclusions

In conclusion, an efficient method has been applied to achieve improved energy density and ultrahigh energy efficiency for ferroelectric materials by doping BZN in tricritical ceramics. The doped BZN can obviously lower the sintering temperature of BTS ceramics. Furthermore, the highest electrical breakdown strength appeared in BTS$_{0.105-y}$BZN ($y$ = 10 wt %), with a value of $E_b$ = 233 kV/cm. On this basis, the relative enhanced energy density reached $U_e$ = 1.15 J/cm$^3$, which may be ascribed to the formation of a merged structure. On the other hand, the relative energy efficiency is more than 99%, which may be related to the tricritical phenomenon. Hence, doping BZN in tricritical ceramics is a significant approach for improving the energy performance for materials.

**Conflicts of Interest:** The authors declare no conflict of interest.

## References

1. Chu, B.J.; Zhou, X.; Ren, K.L.; Neese, B.; Lin, M.R.; Wang, Q.; Bauer, F.; Zhang, Q.M. A Dielectric Polymer with High Electric Energy Density and Fast Discharge Speed. *Science* **2006**, *313*, 334–336. [CrossRef] [PubMed]
2. Elahi, H.; Eugeni, M.; Gaudenzi, P.A. Review on Mechanisms for Piezoelectric-Based Energy Harvesters. *Energies* **2018**, *11*, 1850. [CrossRef]
3. Correia, T.M.; McMillen, M.; Rokosz, M.K.; Weaver, P.M.; Gregg, J.M.; Viola, G.; Cain, M.G. A Lead-Free and High-Energy Density Ceramic for Energy Storage Applications. *J. Am. Ceram. Soc.* **2013**, *96*, 2699–2702. [CrossRef]
4. Ogihara, H.; Randall, C.A.; McKinstry, S.T. High-Energy Density Capacitors Utilizing $0.7BaTiO_3$–$0.3BiScO_3$ Ceramic. *J. Am. Ceram. Soc.* **2009**, *98*, 1719–1724. [CrossRef]
5. Dang, Z.M.; Zheng, M.S.; Zha, J.W. Ferroelectric polymer materials for electric energy storage. *Ferr. Mater. Energy. Appl.* **2018**, *8*, 169–202.
6. Zha, J.W.; Tong, H.; Dang, Z.W. Electrospinning functional fillers/polymer composites with high energy storage. *Dielectr. Polym. Mater. High-Dens. Energy Storage* **2018**, *8*, 289–321.
7. Gao, J.H.; Dai, Y.; Hu, X.H.; Ke, X.Q.; Zhong, L.S.; Li, S.T.; Zhang, L.X.; Wang, Y.; Wang, D.; Wang, Y.; et al. Practical high piezoelectricity in barium titanate ceramics utilizing multiphase convergence with broad structural flexibility. *EPL* **2016**, *115*, 37001. [CrossRef]
8. Gao, J.H.; Hu, X.H.; Wang, Y.; Liu, Y.B.; Zhang, L.X.; Ke, X.Q.; Zhong, L.S.; Zhao, H.; Ren, X.B. Understanding the mechanism of large dielectric response in Pb-free $(1−x)$ Ba $(Zr_{0.2}Ti_{0.8})O_3−x(Ba_{0.7}Ca_{0.3})TiO_3$ ferroelectric ceramics. *Acta Mater.* **2017**, *125*, 177–186. [CrossRef]
9. Gao, J.H.; Wang, Y.; Liu, Y.B.; Hu, X.H.; Ke, X.Q.; Zhong, L.S.; He, Y.T.; Ren, X.B. Enhancing dielectric permittivity for energy-storage devices through tricritical phenomenon. *Sci. Rep.* **2017**, *7*, 40916. [CrossRef]
10. Gao, J.H.; Liu, Y.B.; Wang, Y.; Hu, X.H.; Yan, W.B.; Ke, X.Q.; Zhong, L.S.; He, Y.T.; Ren, X.B. Designing high dielectric permittivity material in barium titanate. *J. Phys. Chem. C* **2017**, *121*, 13106–13113. [CrossRef]
11. Wang, M.J.; Yang, H.; Zhang, Q.L.; Lin, Z.S.; Zhang, Z.S.; Yu, D.; Hu, L. Microstructure and dielectric properties of $BaTiO_3$ ceramic doped with yttrium, magnesium, gallium and silicon for AC capacitor application. *Mater. Res. Bull.* **2014**, *60*, 485–491. [CrossRef]
12. Zhao, Y.Y.; Xu, J.W.; Yang, L.; Zhou, C.R.; Lu, X.P.; Yuan, C.L.; Li, Q.N.; Chen, G.H.; Wang, H. High energy storage property and breakdown strength of $Bi_{0.5}(Na_{0.82}K_{0.18})_{0.5}TiO_3$ ceramics modified by $(Al_{0.5}Nb_{0.5})^{4+}$ complexion. *J. Alloys Compd.* **2016**, *666*, 209–216. [CrossRef]
13. Xie, L.Y.; Huang, X.Y.; Li, B.W.; Zhi, C.Y.; Tanaka, T.; Jiang, P.K. Core–satellite Ag@ $BaTiO_3$ nanoassemblies for fabrication of polymer nanocomposites with high discharged energy density, high breakdown strength and low dielectric loss. *Phys. Chem. Chem. Phys.* **2013**, *15*, 17560–17569. [CrossRef] [PubMed]
14. Young, A.; Hilmas, G.; Zhang, S.C.; Schwartz, R.W. Effect of liquid-phase sintering on the breakdown strength of barium titanate. *J. Am. Ceram. Soc.* **2007**, *90*, 1504–1510. [CrossRef]
15. Qu, B.Y.; Du, H.L.; Yang, Z.T.; Liu, Q.H.; Liu, T.H. Enhanced dielectric breakdown strength and energy storage density in lead-free relaxor ferroelectric ceramics prepared using transition liquid phase sintering. *RSC Adv.* **2016**, *6*, 34381–34389. [CrossRef]
16. Wang, X.R.; Zhang, Y.; Song, X.Z.; Yuan, Z.B.; Ma, T.; Zhang, Q.; Deng, C.S.; Liang, T.X. Glass additive in barium titanate ceramics and its influence on electrical breakdown strength in relation with energy storage properties. *J. Eur. Ceram. Soc.* **2012**, *32*, 559–567. [CrossRef]
17. Zhang, Q.M.; Wang, L.; Luo, J.; Tang, Q.; Du, J. Improved energy storage density in barium strontium titanate by addition of $BaO$–$SiO_2$–$B_2O_3$ glass. *J. Am. Ceram. Soc.* **2009**, *92*, 1871–1873. [CrossRef]
18. Gorzkowski, E.P.; Pan, M.J.; Bender, B.; Wu, C.C.M. Glass-ceramics of barium strontium titanate for high energy density capacitors. *J. Electroceram.* **2007**, *18*, 269–276. [CrossRef]
19. Wang, Y.F.; Cui, J.; Yuan, Q.B.; Niu, Y.J.; Bai, Y.Y.; Wang, H. Significantly enhanced breakdown strength and energy density in sandwich-structured barium titanate/poly(vinylidene fluoride) nanocomposites. *Adv. Mater.* **2015**, *27*, 6658–6663. [CrossRef]
20. Tome, V.; Randall, C.A. High field dielectric properties of anisotropic polymer-ceramic composites. *J. Appl. Phys.* **2008**, *104*, 074106. [CrossRef]

21. Li, J.J.; Claude, J.; Norena-Franco, L.E.; Seok, S.I.; Wang, Q. Electrical Energy Storage in Ferroelectric Polymer Nanocomposites Containing Surface-Functionalized $BaTiO_3$ Nanoparticles. *Chem. Mater.* **2008**, *20*, 6304–6306. [CrossRef]

22. Wu, L.W.; Wang, X.H.; Li, L.T. Lead-free $BaTiO_3–Bi(Zn_{2/3}Nb_{1/3})O_3$ weakly coupled relaxor ferroelectric materials for energy storage. *RSC Adv.* **2016**, *6*, 14273–14282. [CrossRef]

23. Liu, W.H.; Wang, H. Enhanced dielectric properties of $Bi_{1.5}ZnNb_{1.5}O_7$ thick films via cold isostatic pressing. *J. Electroceram.* **2012**, *29*, 183–186. [CrossRef]

24. Liu, W.H.; Wang, H.; Li, K.C.; Zhang, M.H.; Yao, X. $Bi_{1.5}ZnNb_{1.5}O_7$ cubic pyrochlore ceramics prepared by aqueous solution–gel method. *J. Sol-Gel Sci. Technol.* **2009**, *52*, 153–157.

25. Wei, X.Y.; Yao, X. Preparation, structure and dielectric property of barium stannate titanate ceramics. *Mater. Sci. Eng. B* **2007**, *137*, 184–188. [CrossRef]

26. Liu, W.; Wang, H.; Li, K.; Yao, X. Effect of Ag on the sintering and dielectric properties behavior of $Bi_{1.5}ZnNb_{1.5}O_7$ ceramics. *J. Alloys Compd.* **2010**, *491*, 218–222. [CrossRef]

27. Zhao, C.L.; Wu, H.J.; Li, F.; Cai, Y.Q.; Zhang, Y.; Song, D.S.; Wu, J.G.; Lyu, X.; Yin, J.; Xiao, D.Q.; et al. Practical High piezoelectricity in barium titanate ceramics utilizing multiphase convergence with broad structural flexibility. *J. Am. Chem. Soc.* **2018**, *140*, 15252–15260. [CrossRef] [PubMed]

28. Zhang, L.; Lou, X.J.; Wang, D.; Zhou, Y.; Yang, Y.; Kuball, M.; Carpenter, M.A.; Ren, X.B. Glass-glass transitions by means of an acceptor-donor percolating electric-dipole network. *Phys. Rev. Appl.* **2017**, *8*, 054116. [CrossRef]

29. Zhang, L.; Ren, X.B.; Carpenter, M.A. Influence of local strain heterogeneity on high piezoelectricity in $0.5Ba(Zr_{0.2}Ti_{0.8})O_3−0.5(Ba_{0.7}Ca_{0.3})TiO_3$ ceramics. *Phys. Rev. B: Condens. Matter* **2017**, *95*, 054116. [CrossRef]

30. Zheng, L.; Zhang, M.; Wang, L.; Zhou, C.; Zhang, Z.; Yao, Y.G.; Zhang, L.X.; Xue, D.Z.; Lou, X.J.; Ren, X.B. Phase transitions and the piezoelectricity around morphotropic phase boundary in $Ba(Zr_{0.2}Ti_{0.8})O_{3−x}(Ba_{0.7}Ca_{0.3})TiO_3$ lead-free solid solution. *Appl. Phys. Lett.* **2014**, *105*, 162908. [CrossRef]

31. Zheng, T.; Wu, J.G.; Xiao, D.Q.; Zhu, J.G. Recent development in lead-free perovskite piezoelectric bulk materials. *Prog. Mater. Sci.* **2018**, *98*, 552–624. [CrossRef]

32. Roy, C.; Benguigui, L. The tricritical point in $BaTiO3$. *J. Phys. C: Solid State Phys.* **1977**, *10*, 1963.

33. Ramrez, R.; Lapea, M.F.; Gonzalo, J.A. Pressure dependence of free-energy expansion coefficients in $PbTiO_3$ and $BaTiO_3$ and tricritical-point behavior. *Phys. Rev. B: Condens. Matter* **1990**, *42*, 2604. [CrossRef]

34. Rossetti, J.; George, A.; Alexandra, N. Calorimetric investigation of tricritical behavior in tetragonal $Pb(Zr_xTi_{1−x})O_3$. *J. Solid State Chem.* **1999**, *144*, 188–194. [CrossRef]

35. Gao, J.H.; Wang, Y.; He, Z.X.; Liu, Y.B.; Wang, D.; Jin, L.; Zhao, T.X.; Zhong, L.S.; Ren, X.B. Laminated Modulation of Tricritical Ferroelectrics Exhibiting Highly Enhanced Dielectric Permittivity and Temperature Stability. *Adv. Funct. Mater.* **2019**, *1807162*, 1–9. [CrossRef]

36. Li, H.; Liu, F.; Fan, B.; Ai, D.; Peng, Z.; Wang, Q. Nanostructured Ferroelectric-Polymer Composites for Capacitive Energy Storage. *Small Methods* **2018**, *2*, 1700399. [CrossRef]